Desalination and Water Treatment
www.deswater.com

doi: 10.5004/dwt.2020.24913

175 (2020) 316–328
January

Influence of various operating parameters on struvite metastable zone width

Pengfei Wang[a,*], Carsten Meyer[b], Heidrun Steinmetz[c]

[a]*National Engineering Laboratory for Lake Pollution Control and Ecological Restoration, Chinese Research Academy of Environmental Sciences, 100012 Beijing, China, Tel. +86 1084915318; email: wangpf01@craes.org.cn*
[b]*Institute for Sanitary Engineering, Water Quality and Solid Waste Management, University of Stuttgart, Bandtäle 2, 70569 Stuttgart, Germany, Tel. +49 71168563754; email: carsten.meyer@iswa.uni-stuttgart.de*
[c]*Resource Efficient Wastewater Technology, Department of Civil Engineering, University of Kaiserslautern, Paul-Ehrlich-Str. 14, 67663 Kaiserslautern, Germany, Tel. +49 6312052944; email: heidrun.steinmetz@bauing.uni-kl.de*

Received 27 June 2018; Accepted 12 September 2019

ABSTRACT

Struvite metastable zone width (MSZW) is important for the operation of struvite crystallizers to recover phosphorus (P) from wastewater streams as large struvite crystals. However, limited information on struvite MSZW is available. In this study, struvite MSZW was determined under 32 different conditions in a continuously stirred struvite crystallizer to systematically examine the influence of various operating parameters on struvite MSZW. It was found that struvite MSZW (1.3–73.1, presented as a supersaturation ratio difference) broadened with increasing pH (7.6–8.6), struvite seed size (0.3–1.7 mm) and addition rate of $MgCl_2$ solution (0.7–4.1 mg Mg min^{-1}), but narrowed with increasing agitation intensity (Reynolds number = 5.4×10^3–2.3×10^4) and struvite seed mass (0–3.33 g L^{-1}). Based on the results of this study, the supersaturation ratio of struvite in industrial struvite crystallizers should be kept below 10.7 to avoid the intensive formation of fine struvite crystals and the optimal supersaturation ratio is 5.4, under operating conditions similar to those used in this study. When changing the operating parameters of a struvite crystallizer, the resulting change of struvite MSZW should be considered, especially when using the supersaturation ratio as the process controlling parameter. From the MSZW perspective, higher pH, larger addition rate of $MgCl_2$ solution, lower agitation intensity, smaller seed amount or larger struvite seeds enhances the production of large struvite crystals in struvite crystallizers for P recovery from wastewater.

Keywords: Controlling parameter; Metastable zone width; Phosphorus recovery; Struvite crystallization; Supersaturation generation rate

1. Introduction

Various technologies have been developed in the last decades to recover phosphorus (P) from different wastewater streams by struvite ($MgNH_4PO_4 \cdot 6H_2O$) crystallization (Eq. (1)) in fluidized bed reactors [1–3], stirred tank reactors [4–6] and reactors with dual functions of aeration and settling [7–9]. To increase the supersaturation level of struvite in the reactor, Mg sources are generally added to the reactors and the pH is raised by adding a base (e.g. NaOH) or by aeration to strip out the dissolved CO_2 [8]. The recovered struvite is an effective multi-nutrient slow-release fertilizer that gives equivalent P uptake and yield for plants as conventional P fertilizers like di-ammonium phosphate and triple superphosphate [10,11].

$$Mg^{2+} + NH_4^+ + H_nPO_4^{(3-n)-} + 6H_2O \leftrightarrow MgNH_4PO_4 \cdot 6H_2O + nH^+ \quad (1)$$

where n equals 1 or 2 in the pH range 5.5–9.0 [12].

* Corresponding author.

Regardless of the type of reactor, keeping the supersaturation level of struvite in the reactor within the metastable zone (the region between the solubility limit and the supersolubility limit) where nucleation does not take place spontaneously is a prerequisite for the stable operation of the struvite crystallizer and obtaining products with a specific quality regarding crystal size distribution, habit, purity, etc. [13]. Generally, the extent or width of the metastable zone is expressed as the metastable zone width (MSZW). On the one hand, a high supersaturation level exceeding the supersolubility limit of struvite causes intensive nucleation, resulting in small products [14], decreased P recovery efficiency [15] and problematic operation of the struvite crystallizer [16]. On the other hand, a low supersaturation level leads to a small crystal growth rate. Thus, a long crystal retention time is needed to obtain large struvite crystals as products that are easy to harvest, dry quickly and have good properties for transport and application [1]. As a rule of thumb, operating the crystallizer at approximately half of the MSZW of the crystallization system is considered to be optimal [17]. Previous studies have shown that the MSZW of crystals is influenced by many operating parameters of the crystallizers such as the supersaturation generation rate, presence of impurities, seeding, agitation intensity, solution volume, etc. [18,19]. For example, a smaller MSZW is obtained at a smaller supersaturation generation rate or when the crystallization solution is seeded. Therefore, it is critical to determine the MSZW of struvite and the effects of the operating parameters of struvite crystallizers on it to recover P as struvite crystals with expected quality.

Despite the great importance, limited research has focused on the struvite MSZW (Table 1), especially under the conditions typical for operating struvite crystallizers fed with wastewater. Struvite MSZW determined in the previous studies (from 1.8 to 2,511 as a supersaturation ratio difference) differed by three orders of magnitude [20–23]. It was found to be independent of pH [21] but decreased with the increasing agitation rate [22] and ultrasonic power [23]. However, the supersaturation generation and nucleation detection methods, and the forms in which the struvite MSZW was reported (as a pH or concentration difference) varied in these studies, making the interpretation and comparison of the results ambiguous. Moreover, the effects of other operating parameters (supersaturation generation rate, seed mass, etc.) of a struvite crystallizer on the struvite MSZW have not been examined. The purposes of this study are to determine struvite MSZW and systematically investigate the influence of the operating parameters of a struvite crystallizer ($MgCl_2$ solution addition rate, pH, agitation intensity, seed mass, and seed size) on the struvite MSZW.

2. Materials and methods

2.1. Experimental solution and analysis methods

The experiments were conducted with synthetic solutions prepared by dissolving analytical grade chemicals in deionized water. Diammonium hydrogen phosphate ($(NH_4)_2HPO_4$, VWR, Belgium) and ammonium chloride (NH_4Cl, Merck, Germany) were used to prepare the P–N solution with 135 mg L^{-1} orthophosphate-P (PO_4–P) and 610 mg L^{-1} total ammonia nitrogen (TAN). Magnesium chloride hexahydrate ($MgCl_2{\cdot}6H_2O$, Merck, Germany) was used for the $MgCl_2$ solution with 1,380 mg L^{-1} total dissolved Mg. 0.5 and 1.0 M NaOH solutions were also prepared with anhydrous sodium hydroxide (Merck, Germany). The PO_4–P concentration and N:P molar ratio (~10:1) of the P–N solution approximated to the average values of those in the anaerobically digested sludge liquor from wastewater treatment plants using enhanced biological P removal which is the most common wastewater stream for P recovery by struvite crystallization [24]. The $MgCl_2$ solution concentration yielded an Mg:P molar ratio of 1.3:1 at the volume ratio of the $MgCl_2$ solution to the P–N solution of 1:10 which simulated the practical struvite crystallizer operation where a concentrated $MgCl_2$ solution was added to the wastewater at a small rate. The PO_4–P and TAN concentrations of the prepared P–N solution and the total dissolved Mg concentration of the $MgCl_2$ solution were standardized before the experiments. PO_4–P and TAN concentrations were determined with a spectrophotometer (UV-1800, Shimadzu, Germany) according to DIN EN ISO 6878 and DIN 38406-5, respectively. The total dissolved Mg

Table 1
Previous studies on struvite MSZW

References	Supersaturation generation method	Nucleation detection method	pH	Agitation rate (rpm)	MSZW report form	MSZW (ΔS^b)
[20]	pH increase	Visual observation of laser light scattering	–	35	pH difference	2.5–73
[21]	Mg concentration increase	pH drop, visual observation	8.0, 8.5	200	Concentration difference, $SI_{st}{}^a$	71–2,511
[22]	pH increase	pH drop, visual observation	–	50, 100, 120	pH difference	1.8–173
[23]	pH increase	Drop of the laser transmission	–	400	pH difference	0.9–3.6

[a]SI_{st}: supersaturation index of struvite (Eq. (2)).
[b]ΔS: struvite MSZW, expressed as the difference between the supersaturation ratios of struvite (Eq. (3)) at the supersolubility limit and solubility limit. Supersaturation ratios of struvite at the supersolubility limit were calculated from SI_{st} data given in [21] and with PHREEQC interactive based on the concentrations and pH data given in the other three studies.

concentration was determined by titration with an ethylenediaminetetraacetic acid solution.

2.2. Experimental setup and procedure

The MSZW of struvite was experimentally determined by a gradual increase of the supersaturation degree of struvite in the experimental solution until nucleation took place. The gradual increase of struvite supersaturation degree in the experimental solution was realized by dosing $MgCl_2$ solution to the stirred P–N solution at constant pH and temperature, modified from the method of Bhuiyan et al. [21]. All experiments were conducted in a constant temperature room (20°C ± 2°C) [23] with a 1 L glass beaker (inner diameter = 10 cm) stirred with a three-blade marine propeller (diameter = 5 cm) made of stainless steel. The distance from the propeller to the bottom of the beaker was 1.0 cm. A four-blade standard baffle made of stainless steel (dimensions are given in Fig. S1) was inserted in the beaker to facilitate mixing. To detect nucleation and compare different nucleation detection methods, the pH, conductivity and turbidity of the solution in the beaker were recorded (once every 10 s) with the pH (SenTix, WTW, Germany), conductivity (LF 400, GHM-Greisinger, Germany) and turbidity (Ponsel Mesure, France) electrodes and meters (WTW, Germany; GMH 5450, GHM-Greisinger, Germany; Odeon, Ponsel Mesure, France). The electrodes were fixed at the same positions in the beaker in all experiments. A thermometer incorporated in the turbidity meter also recorded the temperature of the solution during the experiments which varied marginally (within 1.0°C) in all experiments.

At the beginning of each experiment, 600 mL P–N solution was filled in the beaker and stirred. The pH of the P–N solution was adjusted to the set value with the NaOH solution. After further stirring for 3 min to ensure a steady-state, a certain volume of $MgCl_2$ solution was added to the beaker from the surface close to the stirrer shaft, followed by immediate addition of NaOH solution until the pH of the mixture in the beaker reached again the initial set value. By doing so, the PO_4–P and TAN concentrations of the mixture in the beaker dropped slightly and the total dissolved Mg concentration increased at the set pH. Consequently, struvite supersaturation degree of the mixture in the beaker increased. After a certain time interval (5–30 min, Table 2), the same volumes of $MgCl_2$ solution and NaOH solution were added to the beaker for the second time, which brought a further increase of struvite supersaturation degree at the set pH. No NaOH solution was added during the interval because the pH of the mixture did not change when no nucleation took place. The addition of the fixed volumes of $MgCl_2$ and NaOH solutions to the beaker after the fixed time interval was repeated until the pH dropped continuously and the turbidity increased dramatically which indicated the occurrence of nucleation. Since the initially formed nuclei could not be detected immediately after their formation due to the tiny sizes, the time interval left between the addition of the solutions allowed the initially formed nuclei to grow to detectable sizes and quantities after the nucleation supersaturation degree (the metastability limit) was reached. In similar experiments for the determination of struvite MSZW, a time interval of 2 or 15 min was also adopted between every step of supersaturation degree increase [20,23]. The mixture in the beaker was continuously stirred during the experiment. Each experiment was repeated at least three times. In the experiments with seeds, the seeds were added to the beaker immediately after the first-time addition of $MgCl_2$ and NaOH solutions to prevent the dissolution of the seeds in the undersaturated P–N solution. Struvite particles of different sizes produced from a previous continuous struvite crystallization experiment with the same solutions as used in this study were separated by sieving and directly used as seeds without grinding.

With the total volume of the $MgCl_2$ solution added in each experiment, the composition of the mixed solution in the beaker at the time of nucleation (the supersolubility limit) was calculated. The supersaturation index of struvite (SI_{st}, Eq. (2) and other minerals at the supersolubility limit were calculated with PHREEQC interactive (Version 3.4.0, USGS) based on the composition and pH. From that, the supersaturation ratio of struvite (S_{st}, Eq. (3) and other minerals were calculated. The calculated S_{st} was the supersaturation ratio of struvite at the supersolubility limit (S_{st}^s). The supersaturation ratio of struvite at equilibrium (S^*) equals 1. The MSZW of struvite (ΔS) was thus S_{st}^s minus 1. The database minteq.v4 of PHREEQC interactive was used for the calculation. The equilibrium with CO_2 in the atmosphere (partial pressure = $10^{-3.4}$ atm) was also considered.

$$SI_{st} = \log_{10}\left(\frac{\alpha_{Mg^{2+}}\alpha_{NH_4^+}\alpha_{PO_4^{3-}}}{K_{sp,st}}\right) \tag{2}$$

$$S_{st} = \frac{\alpha_{Mg^{2+}}\alpha_{NH_4^+}\alpha_{PO_4^{3-}}}{K_{sp,st}} = 10^{SI_{st}} \tag{3}$$

$$Re = \frac{\rho N D^2}{\mu} \tag{4}$$

where SI_{st} and S_{st} are the supersaturation index and supersaturation ratio of struvite respectively, Re is the Reynolds number in the stirred vessel, $\alpha_{Mg^{2+}}$, $\alpha_{NH_4^+}$ and $\alpha_{PO_4^{3-}}$ are the activities of the ions in the solution (mol L^{-1}), ρ is the water density at 20°C (kg m^{-3}), N is the rotational speed of the stirrer (s^{-1}), D is the diameter of the stirrer (m), μ is the dynamic viscosity of water at 20°C (kg m^{-1} s^{-1}), and $K_{sp,st}$ is the thermodynamic solubility product of struvite ($10^{-13.26}$ mol^3 L^{-3} according to Ohlinger et al. [25]). The $K_{sp,st}$ value from Ohlinger et al. [25] was measured at 25°C. Since the temperature has a marginal effect on the $K_{sp,st}$ value between 20°C and 25°C [26], the $K_{sp,st}$ value from Ohlinger et al. [25] was used in the calculation. The solubility products of other minerals included in the database were also used.

2.3. Experimental conditions and statistical analysis

In total, 32 experiments under different conditions were conducted (Table 2). The effects of the addition rate of $MgCl_2$ solution (0.7–4.1 mg Mg min^{-1}), pH (7.6–8.6), agitation intensity (130–560 rpm, corresponding to the Reynolds number

Table 2
Experimental conditions and determined struvite MSZW

Exp.	Addition volume of $MgCl_2$ solution	Addition interval of $MgCl_2$ solution	Addition rate of $MgCl_2$ solution	pH	Agitation rate	Seed size	Seed amount	MSZW (ΔS^a)
	mL	min	mg Mg min^{-1}	–	rpm	mm	g L^{-1}	–
1	2.5	5	0.7	7.6	400	–	–	10.5 ± 0.5
2	3.75	5	1.0	7.6	400	–	–	13.2 ± 0.3
3	5	5	1.4	7.6	400	–	–	14.5
4	7.5	5	2.1	7.6	400	–	–	16.0
5	15	5	4.1	7.6	400	–	–	18.4 ± 0.2
6	15	30	0.7	7.6	400	–	–	9.7
7	15	20	1.0	7.6	400	–	–	12.8
8	15	15	1.4	7.6	400	–	–	15.2
9	15	10	2.1	7.6	400	–	–	16.8
10	10	10	1.4	7.6	400	–	–	13.7 ± 1.0
11	10	10	1.4	7.8	400	–	–	20.4
12	10	10	1.4	8.0	400	–	–	27.2
13	10	10	1.4	8.2	400	–	–	31.4
14	10	10	1.4	8.4	400	–	–	49.1
15	10	10	1.4	8.6	400	–	–	73.1
16	10	10	1.4	7.6	130	–	–	17.2
17	10	10	1.4	7.6	160	–	–	16.7 ± 0.4
18	10	10	1.4	7.6	190	–	–	16.0 ± 0.5
19	10	10	1.4	7.6	220	–	–	15.6 ± 0.5
20	10	10	1.4	7.6	260	–	–	15.4 ± 0.9
21	10	10	1.4	7.6	300	–	–	15.2
22	10	10	1.4	7.6	360	–	–	13.8
23	10	10	1.4	7.6	460	–	–	11.9
24	10	10	1.4	7.6	500	–	–	11.9
25	10	10	1.4	7.6	560	–	–	9.7
26	5	5	1.4	7.6	300	1.4–2.0	0.01	9.7
27	5	5	1.4	7.6	300	1.4–2.0	0.13	6.9
28	5	5	1.4	7.6	300	1.4–2.0	0.67	3.4
29	5	5	1.4	7.6	300	1.4–2.0	1.33	2.0 ± 1.0
30	5	5	1.4	7.6	300	1.4–2.0	3.33	1.3
31	5	5	1.4	7.6	300	0.250–0.355	0.13	2.0 ± 1.0
32	5	5	1.4	7.6	300	0.71–0.80	0.13	5.2

[a]Mean value and standard deviation of the results from three or more repeated experimental runs. Standard deviation equals zero when not shown.

(Re) of 5,400–23,300, Eq. (4)), seed amount (0.01–3.33 g L^{-1}) and seed size (mean size = 0.3–1.7 mm) on struvite MSZW were examined in five groups of experiments respectively, by keeping the investigated parameter as the only variable. The chosen pH and seed size ranges are commonly used in struvite crystallizers for P recovery. The agitation intensity range covered the transition ($10 \le Re \le 1.0 \times 10^4$) and turbulent ($Re > 1.0 \times 10^4$) flow regimes [27] to show the possible different effects on struvite MSZW in different flow regimes. The seed mass ranged from only two particles in the reactor (0.01 g L^{-1}) to a sufficient amount (3.33 g L^{-1}). Except for the seed size, at least five different values of the investigated parameter with equal intervals or slightly larger intervals in the higher value range were tested in each group of experiments. Only three different seed sizes with large intervals were tested because the difference in MSZW between the neighboring experiments would be insignificant with smaller seed size intervals. More than five different values of pH and agitation intensity were tested to show the possible different effects in different value ranges.

In Exp. 1 to Exp. 9, the addition rate of $MgCl_2$ solution was varied either by changing the addition volume (Exp. 1 to Exp. 5) or addition interval (Exp. 5 to Exp. 9), while all the other factors were held constant. These experiments were designed to examine the effect of the addition rate of $MgCl_2$ solution (supersaturation generation rate) on struvite MSZW, as well as to check if the same results could be obtained at the same addition rate with different addition volumes and

intervals. The addition rate of $MgCl_2$ solution in the other experiments was fixed at 1.4 mg Mg min^{-1} (10 mL solution added every 10 min) which was the median value of the tested addition rate range from Exp. 1 to Exp. 9. The addition volume and interval of $MgCl_2$ solution were halved in the experiments with seeds because preliminary experiments showed that struvite nucleated in the majority of the experiments with seeds already after the first addition of 10 mL $MgCl_2$ solution, that is, the supersaturation degree created by the dosage of 10 mL $MgCl_2$ solution exceeded the metastable limit. Only with a smaller addition volume of $MgCl_2$ solution could the struvite MSZW values at different seeding conditions be identified. To keep the same addition rate of $MgCl_2$ solution as in the other experiments, the addition interval of the $MgCl_2$ solution was also halved. The agitation rate in the experiments without seeds was fixed at 400 rpm which ensured a fully turbulent flow regime (Re = 16640) and instant mixing of the added solutions. The agitation rate in the experiments with seeds (300 rpm) was the minimum rate to keep the 3.33 g L^{-1} of 1.4–2.0 mm struvite seeds suspended. Higher agitation rates were not chosen to avoid seed breakage by the stirrer. Generally, a relatively low pH is supposed to prevent excessive nucleation and enable the production of big struvite crystals [2,6,7,28,29]. Therefore, the pH was set at 7.6 in most of the experiments.

The statistical significance of the differences among the struvite MSZW under different conditions was conducted through a one-way analysis of variance followed by Fisher's least significant difference test at a significance level of 0.05. The statistical analysis was conducted with IBM SPSS Statistics.

3. Results and discussion

3.1. Composition of the nuclei

To investigate the influence of operating parameters on the struvite MSZW, a prerequisite for the correct interpretation of the experimental results was that the nuclei formed in all experiments were pure struvite. This was justified by the calculation results from PHREEQC interactive. In 21 of the 32 experiments, the solution at the time of nucleation, when the supersaturation degree was the highest, was supersaturated only with struvite (struvite was the only substance with a positive SI). In the other 11 experiments, the solution at the time of nucleation was supersaturated with newberyite ($MgHPO_4{\cdot}3H_2O$) besides struvite. However, the SI values of newberyite (0.01–0.14) were much smaller than those of struvite (1.19–1.29) in these experiments. Previous research has shown that in solution systems supersaturated with struvite and newberyite, only struvite precipitates when the ratio of the supersaturation ratio of newberyite (S_{ne}) to the supersaturation ratio of struvite (S_{st}) is smaller than 2.0 [30]. The ratio of S_{ne} to S_{st} was smaller than 0.1 in the 11 experiments. Therefore, newberyite was not likely to form in the experiments and the nuclei were pure struvite.

Some microscopic images of the formed nuclei were taken at the end of the experiments without seeds. Fig. 1 shows exemplarily an image of the crystals taken from the reactor at the end of Exp. 12. The nuclei crystals show the typical prismatic (orthorhombic) shape of struvite crystals. The width of these crystals ranges between 4.5 and 26.0 μm. No images of the crystals were taken in the experiments with seeds because it was impossible to differentiate between the newly formed nuclei and the added seeds or the fragments of the added seeds.

3.2. Detection of struvite nucleation

To detect the start of struvite nucleation, suitable parameters for identifying the starting point are needed. Fig. 2 shows the changes in pH, conductivity, and turbidity of the solution in the stirred beaker during an experiment at pH 7.6 (Exp. 5 in Table 2). After each time the $MgCl_2$ solution was added to the beaker, the pH dropped slightly (by 0.01–0.02) due to the acidity of the $MgCl_2$ solution. It was immediately brought back to the set value by adding a small volume of NaOH solution and remained until the next addition of the $MgCl_2$ solution. The conductivity increased by approximately 0.1 mS cm^{-1} after each addition of the $MgCl_2$ solution because new ions were introduced into the solution. The turbidity remained at zero with a few small fluctuations which dropped immediately to zero and could be considered as the background noise. After several times of adding $MgCl_2$ and NaOH solutions (7 times in Fig. 2), the pH dropped rapidly and continuously. Simultaneously, the turbidity increased sharply, indicating the occurrence of struvite nucleation (Eq. (1)). The pH dropped stepwise since a short time interval was needed for the concentration increase of H^+ generated by the struvite crystallization reaction (Eq. (1)) to become detectable by the pH meter. However, the conductivity varied insignificantly with the changing pH and turbidity. The reason was that only a small number of nuclei formed in the solution at the time of nucleation at pH 7.6 with a relatively low supersaturation. The reduction in the concentrations of dissolved ions due to the nuclei formation was too small to cause any significant decrease in the conductivity of the solution. Similarly, in the experiments at pH 7.8 to 8.2, the conductivity of the crystallization solution in the stirred beaker decreased insignificantly at the time of nucleation indicated by the distinct pH drop and turbidity increase. Different observations were made in the experiments at pH 8.4 and 8.6, where the conductivity dropped substantially with the pH drop and turbidity increase (Figs. S2 and S3). The crystallization driving force (supersaturation) of the nucleation solution was high at the high pH. A large number of nuclei formed, leading to a significant drop in the conductivity.

In the experiments with different stirring rates (130–560 rpm) at pH 7.6 (Exp. 16 to Exp. 25, Table 2), it was also observed that the conductivity changed insignificantly at the time of nucleation indicated by the sharp pH drop (stirring rates = 130–560 rpm) and turbidity increase (stirring rates = 260–560 rpm). The turbidity increase weakened at the small stirring rates (130–220 rpm) because the formed nuclei could not be held in suspension. These results show that pH and turbidity are more sensitive than conductivity to indicate the start of struvite nucleation in solutions containing PO_4–P, TAN and dissolved Mg at pH 7.6–8.2. Thus, pH and/or turbidity monitoring is a suitable method for the detection of struvite nucleation.

The experimentally determined MSZW is highly dependent on the method used for the detection of nucleation.

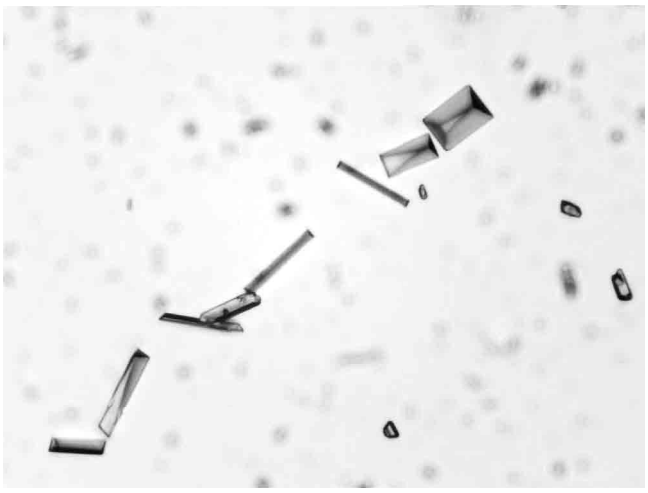

Fig. 1. Microscopic image (magnification factor: 100) of the crystals taken from the reactor at the end of Exp. 12 (conditions: addition rate of $MgCl_2$ solution = 1.4 mg Mg min^{-1}, pH = 8.0, agitation rate = 400 rpm, no seeds).

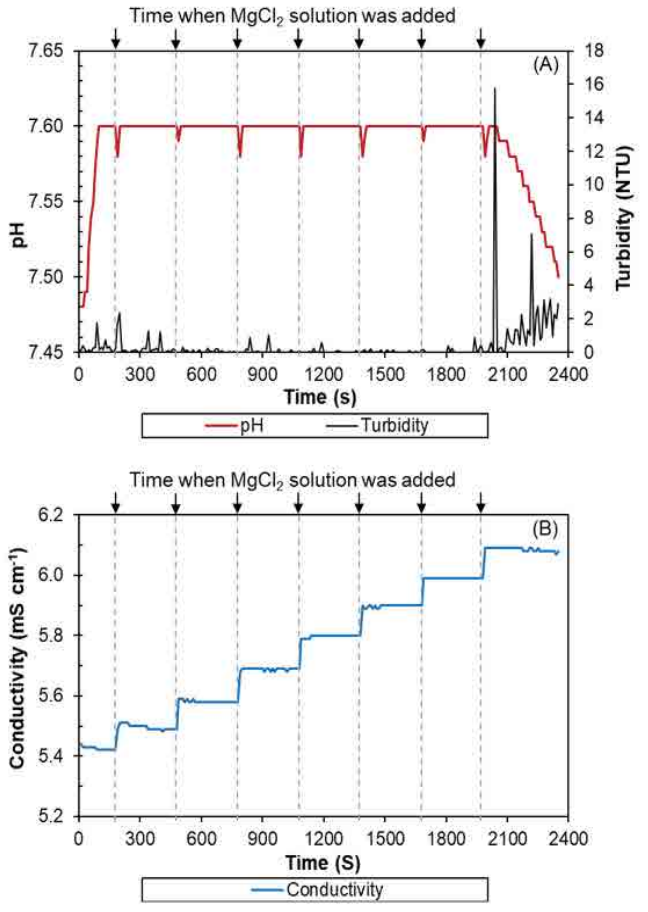

Fig. 2. Typical changes in pH, turbidity (a), and conductivity (b) of the solution in the stirred beaker during an experiment at pH 7.6 (using Exp. 5 as an example, conditions: addition volume of $MgCl_2$ solution = 15 mL, addition interval of $MgCl_2$ solution = 5 min, agitation rate = 400 rpm, no seeds).

Generally, a more sensitive method that depends on the intrinsic properties of the crystallization system leads to an earlier stop of the experiment and smaller MSZW values [31,32]. In the previous studies on struvite MSZW, the nucleation was detected by the drop of pH or laser transmission, or visual observation of the solution color change or laser light scattering in the solution (Table 1). The results of this study confirm that pH monitoring is a sensitive method for the detection of struvite nucleation. However, visual observation is subjective and could vary largely. The inclusion of turbidity monitoring in the experiments of this study provided additional quantitative data, which increased the accuracy of the judgment of the start of nucleation and ensured the accuracy of the experimental results.

3.3. Effect of addition rate of $MgCl_2$ solution (supersaturation generation rate) on struvite MSZW

As shown in Fig. 3a, struvite MSZW values determined from the experiments with varying addition volume (ΔS_v) and addition interval (ΔS_i) of $MgCl_2$ solution were close at the same addition rate. The difference between ΔS_v and ΔS_i at the identical addition rate was between 0.4 and 0.8, originating from the small SI_{st} difference of 0.01 to 0.03. Therefore, changing the added volume and addition interval of the $MgCl_2$ solution did not alter the determined struvite MSZW as long as the addition rate and other factors were maintained.

As the addition rate of $MgCl_2$ solution increased from 0.7 to 4.1 mg Mg min^{-1}, struvite MSZW (ΔS) increased from 10.1 ± 0.5 to 18.4 ± 0.2 ($P < 0.01$), that is, struvite MSZW broadened with a faster addition of $MgCl_2$ solution to the P–N solution, under constant pH (7.6), agitation rate (400 rpm) and without seeds. It was because of the faster addition of $MgCl_2$ solution to the P–N solution increased the supersaturation generation rate (r_s). As the addition rate of the $MgCl_2$ solution increased from 0.7 to 4.1 mg Mg min^{-1}, r_s increased almost linearly (R^2 = 0.97) from 0.16 to 0.43 min^{-1}. r_s in each of the experiments (Exp. 1–Exp. 9) was calculated from a least-square linear regression between the supersaturation ratio of struvite in the mixed solution in the stirred beaker and the time. Except in Exp. 5 (R^2 = 0.92), the coefficients of determination (R^2) of the linear regressions were larger than 0.96, suggesting the good fit of the linear regression to the experimental data.

When $\ln(r_s/min^{-1})$ was plotted against $\ln\Delta S$, a positive linear correlation was obtained, the value of R^2 being 0.93 (Fig. 3b). It directly shows that struvite MSZW increased with an increase in the supersaturation generation rate. In the classical MSZW determination experiments using the polythermal method, the supersaturation of the crystallization solution was generated by cooling. The MSZW was found to increase with an increase of the cooling rate, and there was a linear relationship between the logarithms of the cooling rate and the MSZW for more than 25 substances [33]. This linear relationship has also been observed in recent studies for the cooling crystallization of many inorganic and organic substances such as copper sulfate pentahydrate and salicylic acid [34,35]. In the present study, the supersaturation was generated by the addition of one reactant solution ($MgCl_2$ solution) to the other (P–N solution). The linear relationship between the logarithms of the MSZW and

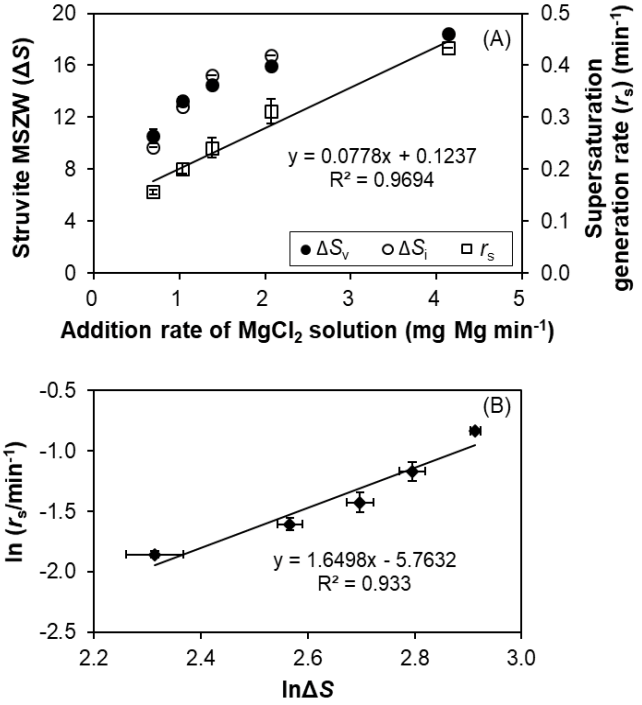

Fig. 3. Effect of the addition rate of $MgCl_2$ solution on struvite MSZW (ΔS) and the supersaturation generation rate (r_s) (a), and the relationship between ln(r_s/min^{-1}) and lnΔS (b). Conditions: pH = 7.6, agitation rate = 400 rpm, no seeds.

the supersaturation generation rate was originally reported for the reactive crystallization of struvite from the aqueous solution. The slope of the linear regression function between lnr_s and lnΔS equals the order of nucleation [33]. According to Fig. 3b, the order of struvite nucleation is 1.6, agreeing with the previous findings that struvite nucleation is a reaction-controlled process and the nucleation order is larger than 1.0 [14].

3.4. Effect of pH on struvite MSZW

Struvite MSZW (ΔS) increased from 13.7 ± 1.0 to 73.1 ($P < 0.01$) as pH increased from 7.6 to 8.6, that is, struvite MSZW broadened at a higher pH, when the addition rate of $MgCl_2$ solution (1.4 mg Mg min^{-1}) and agitation rate (400 rpm) were held constant and no seeds were added to the reactor (Fig. 4). ΔS increased more steeply with pH in the pH range of 8.2–8.6 than in the pH range of 7.6–8.2. A closer look at the activities of the constituent ions of struvite (PO_4^{3-}, NH_4^+ and Mg^{2+}) at the supersolubility limit under the different pH calculated with PHREEQC interactive helps to explain this phenomenon (Fig. 5).

The activities of PO_4^{3-}, NH_4^+ and Mg^{2+} depend on the concentrations of PO_4–P, TAN and total dissolved Mg respectively, as well as the fractions and activity coefficients of the three ions (Eqs. (5)–(7)).

$$\alpha_{PO_4^{3-}} = C_{PO_4-P} \cdot f_{PO_4^{3-}} \cdot \gamma_{PO_4^{3-}} \quad (5)$$

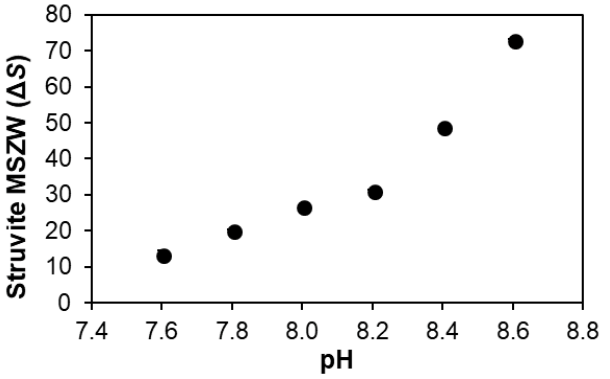

Fig. 4. Effect of pH on struvite MSZW (ΔS). Conditions: addition rate of $MgCl_2$ solution = 1.4 mg Mg min^{-1}, agitation rate = 400 rpm, no seeds.

$$\alpha_{NH_4^+} = C_{TAN} \cdot f_{NH_4^+} \cdot \gamma_{NH_4^+} \quad (6)$$

$$\alpha_{Mg^{2+}} = C_{diss.Mg} \cdot f_{Mg^{2+}} \cdot \gamma_{Mg^{2+}} \quad (7)$$

where C_{PO_4-P}, C_{TAN} and $C_{diss.Mg}$ are the concentrations of PO_4–P, TAN and total dissolved Mg respectively (mol L^{-1}); $f_{PO_4^{3-}}$, $f_{NH_4^+}$ and $f_{Mg^{2+}}$ are the fractions of PO_4^{3-} in PO_4–P, NH_4^+ in TAN and Mg^{2+} in total dissolved Mg respectively; and $\gamma_{PO_4^{3-}}$, $\gamma_{NH_4^+}$ and $\gamma_{Mg^{2+}}$ are the activity coefficients of PO_4^{3-}, NH_4^+ and Mg^{2+} respectively. For a convenient demonstration of the changes of these parameters in the pH range of 7.6–8.6, the relative values of the parameters were calculated by dividing the values of them at different pH to the corresponding values at pH 7.6.

Among the three ions, the activity of PO_4^{3-} changed most greatly with the pH due to the substantial increase of the fraction of PO_4^{3-} in PO_4–P at the higher pH. As shown in Figs. 5a and b, the relative concentrations of PO_4–P and TAN at the supersolubility limit increased from 1.0 at pH 7.6 to 1.05 at pH 8.2 and remained unchanged in the pH range of 8.2 to 8.6. Since the higher pH stimulates the transformation of HPO_4^{2-} and $H_2PO_4^-$ into PO_4^{3-}, the relative fraction of PO_4^{3-} in PO_4–P increased exponentially (R^2 = 0.9985) from 1.0 at pH 7.6 to 13.6 at pH 8.6, resulting in an exponential increase of the relative activity of PO_4^{3-}, with an almost constant activity coefficient of PO_4^{3-} (0.166–0.171). The higher pH favors the transformation of NH_4^+ into NH_3. Therefore, the relative fraction of NH_4^+ in TAN decreased gradually from 1.0 at pH 7.6 to 0.9 at pH 8.6. The activity coefficient of NH_4^+ remained almost constant at 0.8. The overall effect of the changing TAN concentration, NH_4^+ fraction and NH_4^+ activity coefficient was that the relative activity of NH_4^+ at the supersolubility limit increased slightly from 1.0 at pH 7.6 to 1.02 at pH 8.0 but decreased to 1.01 at pH 8.2 and further to 0.94 at pH 8.6. Similarly, the activity coefficient of Mg^{2+} remained almost unchanged (0.45). However, the relative concentration of total dissolved Mg at the supersolubility limit decreased largely from 1.0 at pH 7.6 to 0.4 at pH 8.2 and remained at a higher pH (Fig. 5c). Together with a slight

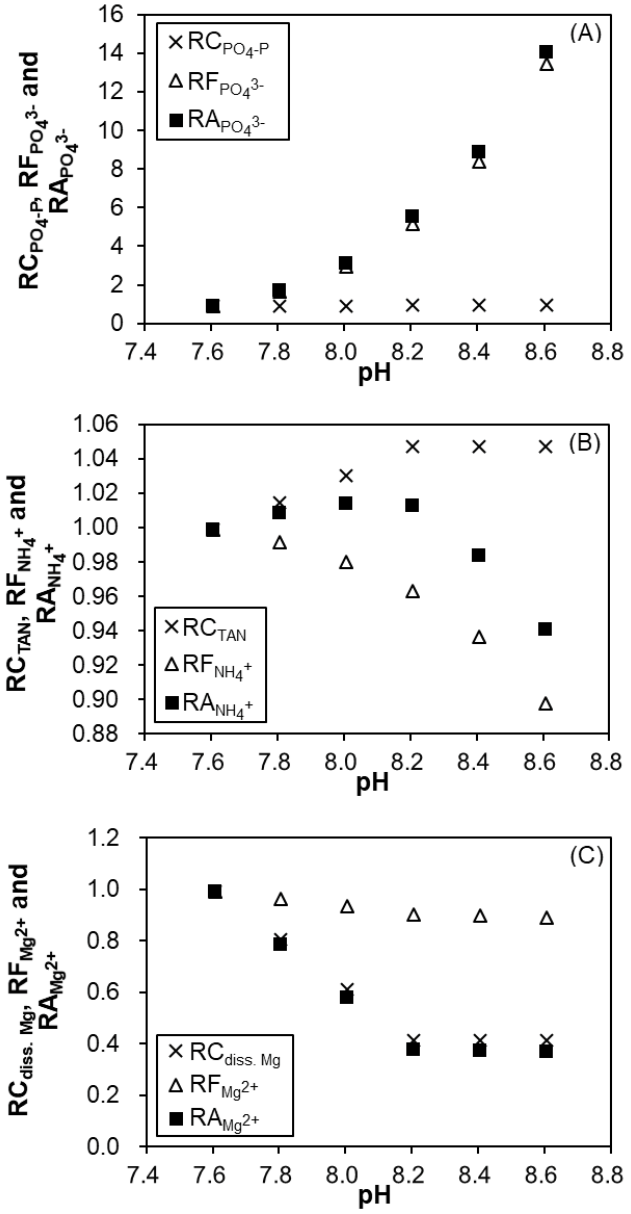

Fig. 5. Relative concentration of PO_4–P (RC_{PO_4-P}), relative fraction of PO_4^{3-} in PO_4–P ($RF_{PO_4^{3-}}$) and relative activity of PO_4^{3-} ($RA_{PO_4^{3-}}$) (a), relative concentration of TAN (RC_{TAN}), relative fraction of NH_4^+ in TAN ($RF_{NH_4^+}$) and relative activity of NH_4^+ ($RA_{NH_4^+}$) (b), and relative concentration of total dissolved Mg ($RC_{diss.Mg}$), relative fraction of Mg^{2+} in total dissolved Mg ($RF_{Mg^{2+}}$) and relative activity of Mg^{2+} ($RA_{Mg^{2+}}$) at the supersolubility limit at different pH.

reduction of the fraction of Mg^{2+} in total dissolved Mg, the relative activity of Mg^{2+} dropped from 1.0 at pH 7.6 to 0.38 at pH 8.2 and remained almost unchanged in the pH range of 8.2 to 8.6. The overall effect of the varying activities of PO_4^{3-}, NH_4^+ and Mg^{2+} at the different pH was that the relative ionic activity product (IAP) of PO_4^{3-}, NH_4^+ and Mg^{2+} at the supersolubility limit increased from 1.0 at pH 7.6 to 2.2 at pH 8.2 and 5.0 at pH 8.6, that is, IAP at the supersolubility limit and thus ΔS (Eq. (2)) increased more steeply with the increasing pH in the pH range of 8.2–8.6.

Our finding that struvite MSZW broadened with the increasing pH was contrary to that of Bhuiyan et al. [21] who stated that struvite MSZW was independent of pH (8.0 and 8.5). In their study, struvite supersolubility and solubility limits were graphically represented as $-\log_{10}\left(\alpha_{PO_4^{3-}}\cdot\alpha_{NH_4^+}\right)$ vs. $-\log_{10}\left(\alpha_{Mg^{2+}}\right)$. The two limits were parallel regardless of pH. When our data were presented in the same way, the region between the two limits which is the MSZW broadened with the increasing pH (Fig. 6). The theory that struvite crystals possess more negative surface charges at a higher pH [36] supports our finding. At the higher pH, the contact and agglomeration of struvite clusters to form nuclei become more difficult due to higher electrostatic repulsions, which finally leads to the broadening of struvite MSZW. Sahin et al. [37] also reported that the MSZW of ammonium biborate tetrahydrate produced by the reaction of ammonium hydroxide with boric acid in aqueous solution increased with the rising pH.

3.5. Effect of agitation intensity on struvite MSZW

Under the experimental conditions (addition rate of $MgCl_2$ solution = 1.4 mg Mg min^{-1}, pH = 7.6, no seeds), struvite MSZW (ΔS) decreased almost linearly (R^2 = 0.96) from 17.2 to 9.7 ($P < 0.01$) as the Reynolds number (Re) increased from 5.4×10^3 to 2.3×10^4, that is, struvite MSZW narrowed at a larger agitation intensity (Fig. 7). The relationship between ΔS and Re was:

$$\Delta S = -3.8\times10^{-4}\,\mathrm{Re} + 19.3 \quad 5.4\times10^3 \le \mathrm{Re} \le 2.3\times10^4 \tag{8}$$

The flow in a stirred vessel is fully turbulent at $Re > 1.0 \times 10^4$. Transition flow occurs at $10 \le Re \le 1.0 \times 10^4$ [27]. For the experimental system of this study, the flow in the stirred beaker became fully turbulent when the agitation rate was larger than 240 rpm (Eq. (4)). No significant difference existed in the relationships between ΔS and Re in the transition flow regime and turbulent flow regime.

Ariyanto [22] also reported that struvite MSZW narrowed with the increasing agitation rate (50, 100, and 120 rpm); however, no correlation between the MSZW and the agitation rate was shown. The negative linear relationship between struvite MSZW and the agitation intensity (Eq. (7)) was originally found in our study. These observations suggest that the primary struvite nucleation is promoted by the increased agitation intensity, that is, when the struvite crystallizer is operated at a higher agitation intensity, the maximum allowable supersaturation level to avoid the massive formation of fine crystals becomes smaller. However, when the agitation intensity exceeds a certain limit, nucleation could be retarded [38]. This limit was not reached in the studied range.

3.6. Effects of seed mass and seed size on struvite MSZW

Struvite MSZW (ΔS) decreased from 9.7 to 1.3 ($P < 0.01$) as the mass density of 1.4–2.0 mm struvite seeds in the reactor

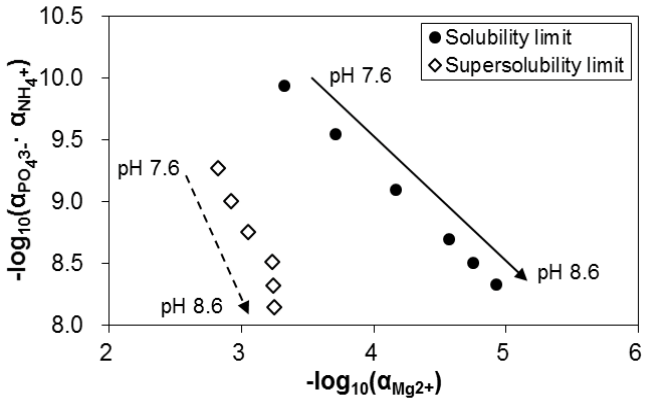

Fig. 6. Struvite solubility and supersolubility limits expressed as $-\log_{10}(\alpha_{PO_4^{3-}} \cdot \alpha_{NH_4^+})$ vs. $-\log_{10}(\alpha_{Mg^{2+}})$ at different pH.

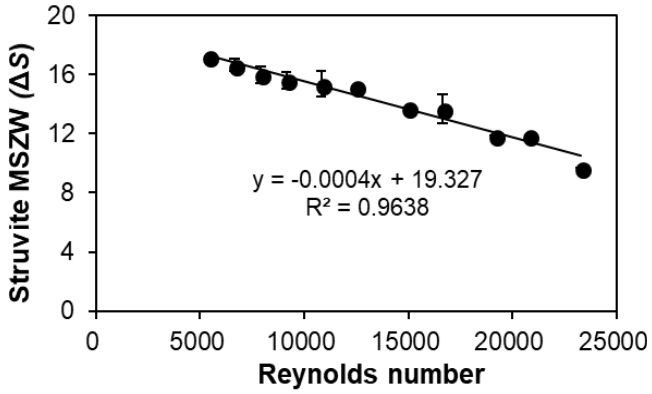

Fig. 7. Effect of agitation intensity on struvite MSZW. Conditions: addition rate of $MgCl_2$ solution = 1.4 mg Mg min^{-1}, pH = 7.6, no seeds.

increased from 0.01 to 3.33 g L^{-1}, that is, struvite MSZW narrowed with more struvite seeds being added to the reactor, at constant seed size, addition rate of $MgCl_2$ solution (1.4 mg Mg min^{-1}, 5 mL $MgCl_2$ solution every 5 min), pH (7.6) and agitation rate (300 rpm) (Fig. 8a, circular data points). This effect was more significant with a smaller amount of seeds (< 0.67 g L^{-1}). The mechanism behind the observed seed mass effect was that more nuclei were generated by the secondary nucleation when more struvite seeds were added to the reactor. The triangular data point in Fig. 8a represents ΔS from the experiment with no seeds under the same operating conditions except that 10 mL $MgCl_2$ solution was added every 10 min (Exp. 21 in Table 2). Since changing the added volume and interval of $MgCl_2$ solution did not affect ΔS at the same addition rate (Fig. 3a), the result of Exp. 21 could be compared with the others in Fig. 8a. With no seeds in the reactor, ΔS was 15.2. When a small number of seeds (0.01 g L^{-1}, two particles) were added, ΔS dropped significantly (by 36%) to 9.7, in agreement with the fact that the secondary nucleation requires a much smaller supersaturation than the primary nucleation.

When the seed mass density (0.13 g L^{-1}) and other conditions (addition rate of $MgCl_2$ solution = 1.4 mg Mg min^{-1}, pH = 7.6, agitation rate = 300 rpm) were kept constant, struvite MSZW (ΔS) increased from 2.0 ± 1.0 to 6.9 ($P < 0.01$) as the mean size of struvite seeds increased from 0.3 to 1.7 mm, that is, struvite MSZW broadened with larger seeds at a constant seed mass (Fig. 8b). The uncertainty of ΔS at the mean seed size of 0.3 mm was high because a large number of small seeds impeded the turbidity measurement. The secondary nucleation rate (number of secondary nuclei produced per unit time and volume) depends on the seed number density, seed size, agitation rate and supersaturation level [39]. Although a larger seed crystal has higher contact energy and more secondary nuclei could be generated by the contact nucleation of the single larger crystal, the total number of larger seed crystals was smaller at the constant seed mass. The overall effect of the increased seed size from 0.3 mm to

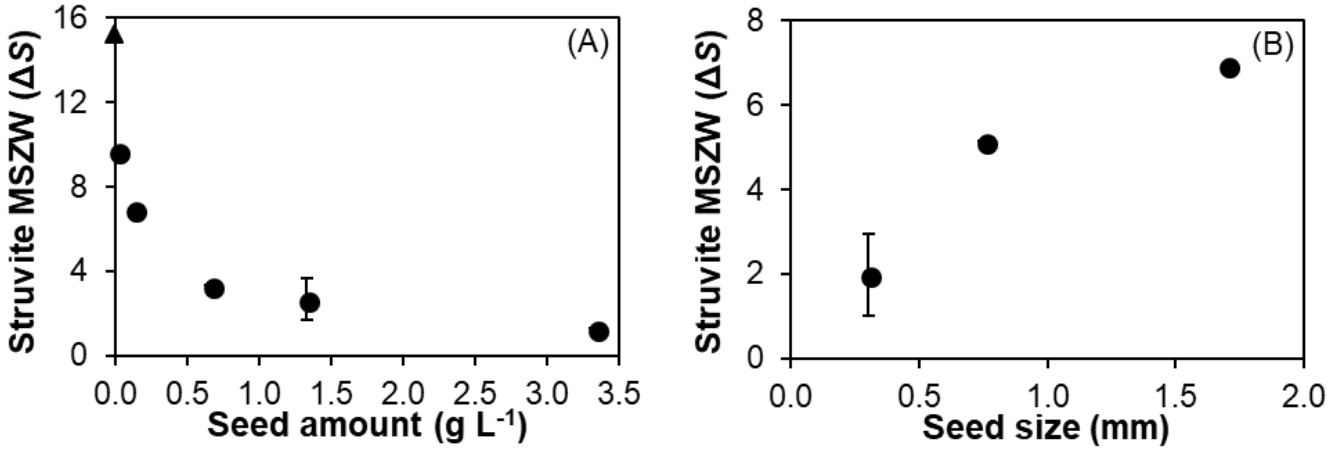

Fig. 8. Effect of seed amount (a) and seed size (b) on struvite MSZW. Conditions: (a) addition rate of $MgCl_2$ solution = 1.4 mg Mg min^{-1}, pH = 7.6, agitation rate = 300 rpm, seed size = 1.4–2.0 mm, the circular data points represent results from the experiments with seeds where 5 mL $MgCl_2$ solution was added every 5 min, the triangular data point represents the result from the experiment without seeds under identical conditions except that 10 mL $MgCl_2$ solution was added every 10 min; (b) addition rate of $MgCl_2$ solution = 1.4 mg Mg min^{-1}, pH = 7.6, agitation rate = 300 rpm, seed mass density = 0.13 g L^{-1}.

1.7 mm was a decreased secondary nucleation rate at the constant seed mass, agitation rate and supersaturation level (detailed calculations can be found in the Supplementary Material). In other words, when the larger seeds were added to the identical crystallization solution (S_{st} = 2.3 after the first-time addition of 5 mL $MgCl_2$ solution), a smaller number of secondary nuclei were formed. Since the pH drop and turbidity increase were related to the number of nuclei, the smaller number of nuclei needed a longer time to increase to the limit which caused significant pH and turbidity changes, that is, the nucleation was detected at a later time (with more addition times of $MgCl_2$ solution) with the larger seeds. Therefore, the experimentally determined MSZW of struvite broadened as the seed crystal size increased.

3.7. Implications for the operation of struvite crystallizers

Struvite MSZW (ΔS) determined from the experiments without seeds ranged between 9.7 and 73.1 in this study (Table 2). It is much smaller than that found by Bhuiyan et al. [21] and within those determined by Ali and Schneider [20] and Ariyanto [22], but larger than that described in Qiu et al. [23] (Table 1). As shown by those previous studies, struvite MSZW varies with the initial PO_4–P concentration of the P–N solution. Besides, the MSZW determined with different nucleation detection techniques could vary substantially [31,40]. These factors and the different experimental conditions (supersaturation generation rate, pH, agitation rate, etc.) all contribute to the different struvite MSZW found in the different studies, so that a clear dependency of struvite MSZW on the operating parameters could not be identified unless the operating conditions are specified.

With the presence of 0.01–3.33 g L^{-1} 1.4–2.0 mm struvite seeds or 0.13 g L^{-1} struvite seeds of three different sizes in the reactor, ΔS decreased to 1.3–9.7 at constant pH (7.6), agitation rate (300 rpm) and addition rate of $MgCl_2$ solution (1.4 mg Mg min^{-1}). Small struvite particles are the most commonly used seed material in struvite crystallizers for P recovery [41]. For the design and operation of industrial crystallizers, the MSZW should be determined in the presence of a small amount of the to be produced material as seeds [13]. Based on the result from the experiment with two 1.4–2.0 mm struvite seed particles (Exp. 26 in Table 2), the supersaturation ratio of struvite in the struvite crystallizer should be kept smaller than 10.7 (ΔS plus 1) to avoid intensive secondary nucleation and produce large struvite crystals. The optimal supersaturation ratio at which the struvite crystallizer should be operated (at half of the MSZW) was approx. 5.4, under operating conditions (pH, agitation intensity, $MgCl_2$ solution addition rate, etc.) similar to those used in this study.

The variation of struvite MSZW and thus the optimal supersaturation ratio with the operating parameters has so far not been systematically studied and been neglected by the operators of struvite crystallizers for P recovery from wastewater. Supersaturation ratio was used as the process controlling parameter by some researchers in operating struvite crystallizers for P recovery [42,43]. Specifically, the optimal supersaturation ratio of struvite in the crystallizer to reach a high P recovery efficiency and obtain good quality products was kept constant. To maintain this optimal supersaturation ratio, the operating parameters such as pH, Mg:P molar ratio and recirculation flow rate were adjusted, when the characteristics of the inflowing wastewater changed. Nevertheless, it is clearly shown in this study that once the operating conditions (pH, agitation intensity, supersaturation generation rate, etc.) change, struvite MSZW and thus the optimal supersaturation ratio change accordingly, especially for pH. When the pH increased slightly from 8.2 to 8.4, struvite MSZW increased by more than 50%, that is, the optimal supersaturation ratio shifted to a much larger value when the other factors were held constant. For the steady crystallizer operation and large size struvite products, a wider MSZW (a higher supersolubility limit) is preferred because the crystallizer can be operated within a broad window and at higher supersaturation levels without the obstructing problem of massive formation of fine crystals [44]. Based on the results of the present study, larger addition rate of $MgCl_2$ solution, higher operation pH, smaller agitation rate, a smaller amount of seeds or larger seeds shifts the supersolubility limit to a higher value and is beneficial for the steady operation of struvite crystallizers and obtaining large struvite products. When two or more of these operating parameters change simultaneously in the positive-effect direction (leading to a higher supersolubility limit), they exert an overall positive effect on the stable operation of struvite crystallizers and the production of large struvite crystals. However, if the operating parameters do not change simultaneously in the positive-effect direction, the effects that may occur cannot be determined based on the results from the present study and further research is needed.

4. Conclusions

pH and turbidity are more sensitive than conductivity to indicate the start of struvite nucleation. pH and turbidity monitoring can be used as the nucleation detection method in further investigations of struvite MSZW. Struvite MSZW (1.3–73.1 as a supersaturation ratio difference) broadens with increasing pH (7.6–8.6), struvite seed size (0.3–1.7 mm) and addition rate of $MgCl_2$ solution (0.7–4.1 mg Mg min^{-1}). It narrows with increasing agitation intensity ($Re = 5.4 \times 10^3$–2.3×10^4) and struvite seed mass (0–3.33 g L^{-1}). These operating parameters of a struvite crystallizer impede or stimulate the tendency or rate of primary or secondary struvite nucleation, resulting in the observed effects on struvite MSZW. The supersaturation ratio of struvite in the industrial struvite crystallizers should be kept below 10.7 to avoid the intensive formation of fine struvite crystals and the optimal supersaturation ratio is 5.4, under operating conditions similar to those used in this study. When operating struvite crystallizers to recover P from wastewater, the variations of struvite MSZW and the optimal supersaturation ratio (at approx. half of the MSZW) with these operating parameters should be taken into account, especially when using the supersaturation ratio as the process controlling parameter. From the MSZW perspective, higher pH, larger addition rate of $MgCl_2$ solution, smaller agitation rate, smaller seed amount or larger struvite seeds can be used to enhance the production of large struvite crystals in struvite crystallizers for P recovery from wastewater.

Acknowledgments

The authors would like to thank the Willy-Hager-Stiftung and Carl-Zeiss-Stiftung for sponsoring the experimental cost and the doctoral scholarship for Pengfei Wang, respectively.

References

[1] K.P. Fattah, D.S. Mavinic, F.A. Koch, Influence of process parameters on the characteristics of struvite pellets, J. Environ. Eng., 138 (2012) 1200–1209.
[2] Q. Ping, Y.M. Li, X.H. Wu, L. Yang, L. Wang, Characterization of morphology and component of struvite pellets crystallized from sludge dewatering liquor: effects of total suspended solid and phosphate concentrations, J. Hazard. Mater., 310 (2016) 261–269.
[3] Y.-J. Shih, R.R.M. Abarca, M.D.G. de Luna, Y.-H. Huang, M.-C. Lu, Recovery of phosphorus from synthetic wastewaters by struvite crystallization in a fluidized-bed reactor: effects of pH, phosphate concentration and coexisting ions, Chemosphere, 173 (2017) 466–473.
[4] S.G. Barbosa, L. Peixoto, B. Meulman, M.M. Alves, M.A. Pereira, A design of experiments to assess phosphorous removal and crystal properties in struvite precipitation of source separated urine using different Mg sources, Chem. Eng. J., 298 (2016) 146–153.
[5] D. Crutchik, J.M. Garrido, Kinetics of the reversible reaction of struvite crystallisation, Chemosphere, 154 (2016) 567–572.
[6] N. Hutnik, A. Kozik, A. Mazienczuk, K. Piotrowski, B. Wierzbowska, A. Matynia, Phosphates (V) recovery from phosphorus mineral fertilizers industry wastewater by continuous struvite reaction crystallization process, Water Res., 47 (2013) 3635–3643.
[7] E. Tarragó, S. Puig, M. Ruscalleda, M.D. Balaguer, J. Colprim, Controlling struvite particles' size using the up-flow velocity, Chem. Eng. J., 302 (2016) 819–827.
[8] Y.-H. Song, G.-L. Qiu, P. Yuan, X.-Y. Cui, J.-F. Peng, P. Zeng, L. Duan, L.-C. Xiang, F. Qian, Nutrients removal and recovery from anaerobically digested swine wastewater by struvite crystallization without chemical additions, J. Hazard. Mater., 190 (2011) 140–149.
[9] K. Suzuki, Y. Tanaka, T. Osada, M. Waki, Removal of phosphate, magnesium and calcium from swine wastewater through crystallization enhanced by aeration, Water Res., 36 (2002) 2991–2998.
[10] P.J. Talboys, J. Heppell, T. Roose, J.R. Healey, D.L. Jones, P.J.A. Withers, Struvite: a slow-release fertiliser for sustainable phosphorus management?, Plant Soil, 401 (2016) 109–123.
[11] R. Cabeza, B. Steingrobe, W. Römer, N. Claassen, Effectiveness of recycled P products as P fertilizers, as evaluated in pot experiments, Nutr. Cycling Agroecosyst., 91 (2011) 173–184.
[12] R. Boistelle, F. Abbona, Nucleation of struvite ($MgNH_4PO_4 \cdot 6H_2O$) single crystals and aggregates, Cryst. Res. Technol., 20 (1985) 133–140.
[13] J.W. Mullin, Crystallization, 4th ed., Elsevier Butterworth-Heinemann, Oxford, 2001.
[14] C.M. Mehta, D.J. Batstone, Nucleation and growth kinetics of struvite crystallization, Water Res., 47 (2013) 2890–2900.
[15] K. Shimamura, T. Tanaka, Y. Miura, H. Ishikawa, Development of a high-efficiency phosphorus recovery method using a fluidized-bed crystallized phosphorus removal system, Water Sci. Technol., 48 (2003) 163–170.
[16] A. Adnan, M. Dastur, D.S. Mavinic, F.A. Koch, Preliminary investigation into factors affecting controlled struvite crystallization at the bench scale, J. Environ. Eng. Sci., 3 (2004) 195–202.
[17] S. Titiz-Sargut, J. Ulrich, Application of a protected ultrasound sensor for the determination of the width of the metastable zone, Chem. Eng. Process. Process Intensif., 42 (2003) 841–846.
[18] T.L. Threlfall, S.J. Coles, A perspective on the growth-only zone, the secondary nucleation threshold and crystal size distribution in solution crystallisation, CrystEngComm., 18 (2016) 369–378.
[19] H.Y. Yang, Relation between metastable zone width and induction time of butyl paraben in ethanol, CrystEngComm., 17 (2015) 577–586.
[20] I. Ali, P.A. Schneider, Crystallization of struvite from metastable region with different types of seed crystal, J. Non-Equilib. Thermodyn., 30 (2005) 95–111.
[21] M.I.H. Bhuiyan, D.S. Mavinic, R.D. Beckie, Nucleation and growth kinetics of struvite in a fluidized bed reactor, J. Cryst. Growth, 310 (2008) 1187–1194.
[22] E. Ariyanto, Crystallisation and Dissolution Studies of Struvite in Aqueous Solutions, Curtin University, Perth, Western Australia, 2013.
[23] L.P. Qiu, L. Shi, Z. Liu, K. Xie, J.B. Wang, S.B. Zhang, Q.Q. Song, L.Q. Lu, Effect of power ultrasound on crystallization characteristics of magnesium ammonium phosphate, Ultrason. Sonochem., 36 (2017) 123–128.
[24] C. Sartorius, J. von Horn, F. Tettenborn, Phosphorus recovery from wastewater—expert survey on present use and future potential, Water Environ. Res., 84 (2012) 313–322.
[25] K.N. Ohlinger, T.M. Young, E.D. Schroeder, Predicting struvite formation in digestion, Water Res., 32 (1998) 3607–3614.
[26] M. Hanhoun, L. Montastruc, C. Azzaro-Pantel, B. Biscans, M. Frèche, L. Pibouleau, Temperature impact assessment on struvite solubility product: a thermodynamic modeling approach, Chem. Eng. J., 167 (2011) 50–58.
[27] R.R. Hemrajani, G.B. Tatterson, Mechanically Stirred Vessels, Chapter 6, E.L. Paul, V.A. Atiemo-Obeng, S.M. Kresta, Eds., Handbook of Industrial Mixing: Science and Practice, John Wiley & Sons, Inc., New Jersey, 2004, p. 361.
[28] L. Egle, H. Rechberger, M. Zessner, Overview and description of technologies for recovering phosphorus from municipal wastewater, Resour. Conserv. Recycl., 105 (2015) 325–346.
[29] M. Ronteltap, M. Maurer, R. Hausherr, W. Gujer, Struvite precipitation from urine – influencing factors on particle size, Water Res., 44 (2010) 2038–2046.
[30] F. Abbona, H.E. Lundager Madsen, R. Boistelle, Crystallization of two magnesium phosphates, struvite and newberyite: effect of pH and concentration, J. Cryst. Growth, 57 (1982) 6–14.
[31] N. Kubota, A new interpretation of metastable zone widths measured for unseeded solutions, J. Cryst. Growth, 310 (2008) 629–634.
[32] L.-D. Shiau, The influence of solvent on the pre-exponential factor and interfacial energy based on the metastable zone width data, CrystEngComm., 18 (2016) 6358–6364.
[33] J. Nývlt, Kinetics of nucleation in solutions, J. Cryst. Growth, 3–4 (1968) 377–383.
[34] E. Lyall, P. Mougin, D. Wilkinson, K.J. Roberts, In situ ultrasonic spectroscopy study of the nucleation and growth of copper sulfate pentahydrate batch crystallized from supersaturated aqueous solutions, Ind. Eng. Chem. Res., 43 (2004) 4947–4956.
[35] D. Mealey, D.M. Croker, Å.C. Rasmuson, Crystal nucleation of salicylic acid in organic solvents, CrystEngComm., 17 (2015) 3961–3973.
[36] K.S. Le Corre, E. Valsami-Jones, P. Hobbs, S.A. Parsons, Kinetics of struvite precipitation: effect of the magnesium dose on induction times and precipitation rates, Environ. Technol., 28 (2007) 1317–1324.
[37] O. Sahin, M. Ozdemir, M.S. Izgp, H. Demir, A.A. Ceyhan, Determination of nucleation kinetics of ammonium biborate tetrahydrate, Rev. Chim., 65 (2014) 1–5.
[38] K.P. Liang, G. White, D. Wilkinson, L.J. Ford, K.J. Roberts, W.M.L. Wood, Examination of the process scale dependence of L-glutamic acid batch crystallized from supersaturated aqueous solutions in relation to reactor hydrodynamics, Ind. Eng. Chem. Res., 43 (2004) 1227–1234.
[39] L. Bauer, R.W. Rousseau, W.L. McCabe, Influence of crystal size on the rate of contact nucleation in stirred-tank crystallizers, AIChE J., 20 (1974) 653–659.
[40] N. Gherras, G. Fevotte, Comparison between approaches for the experimental determination of metastable zone width: a case study of the batch cooling crystallization of ammonium oxalate in water, J. Cryst. Growth, 342 (2012) 88–98.

[41] S. Kataki, H. West, M. Clarke, D.C. Baruah, Phosphorus recovery as struvite: recent concerns for use of seed, alternative Mg source, nitrogen conservation and fertilizer potential, Resour. Conserv. Recycl., 107 (2016) 142–156.
[42] A. Adnan, F.A. Koch, D.S. Mavinic, Pilot-scale study of phosphorus recovery through struvite crystallization — II: applying in-reactor supersaturation ratio as a process control parameter, J. Environ. Eng. Sci., 2 (2003) 473–483.
[43] K. Shimamura, I. Hirasawa, H. Ishikawa, T. Tanaka, Phosphorus recovery in a fluidized bed crystallization reactor, J. Chem. Eng. Jpn., 39 (2006) 1119–1127.
[44] S.S. Kadam, S.A. Kulkarni, R.C. Ribera, A.I. Stankiewicz, J.H. ter Horst, H.J.M. Kramer, A new view on the metastable zone width during cooling crystallization, Chem. Eng. Sci., 72 (2012) 10–19.

Supplementary information

S1. Explanation on the effect of seed size on struvite MSZW

Contact secondary nucleation rate (B, number of secondary nuclei produced per min) could be expressed as the product of the contact nucleation rate with a single seed crystal (B_L, number of secondary nuclei produced per min per seed crystal of size L, μm) and the number of seed crystals in the reactor (N_L) (Bauer et al. [39]):

$$B = B_L N_L \tag{S1}$$

According to Bauer et al. [39], B_L increased with the increasing seed crystal size at the same agitation rate (350 rpm) and supersaturation level:

$$B_L = 0.054L - 4.25\times10^{-6}L^2 \tag{S2}$$

which was due to the increased contact energy of the larger seed crystal.

In the present experiments, the mass of seed crystals was kept constant. Assuming that the seed crystals of all sizes were of the same shape (volume shape factor f_V was a constant) and porosity (ε_p), the number of the seed crystal was inversely proportional to the seed size to the power of 3:

$$N_L = \frac{M_0}{f_v \rho_c \left(1-\varepsilon_p\right) L^3} \tag{S3}$$

where M_0 is the seed mass (0.08×10^{-3} kg); ϱ_c is the true density of struvite (1711 kg m^{-3}); f_V is simplified to that of the sphere ($\pi/6$); ε_p is simplified to 0, and L is in m.

Taking Eqs. (S2) and (S3) into Eq. (S1), B was calculated to be 51,442; 7,957; and 1,445 min^{-1} for seed crystals of 0.30, 0.76, and 1.7 mm, respectively. The secondary nucleation rate decreased with the increasing seed crystal size when the seed mass and experimental conditions were kept constant. Therefore, struvite MSZW broadened as the seed crystal size increased.

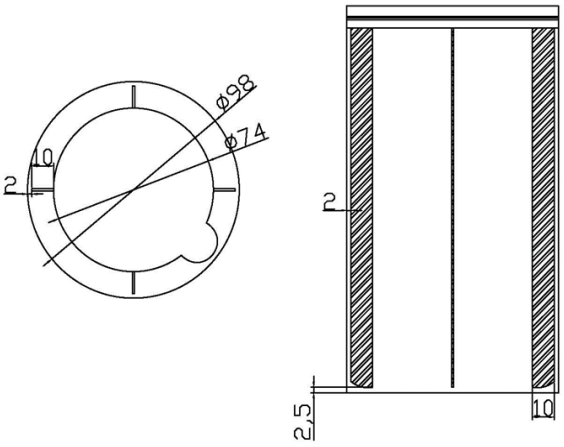

Fig. S1. Dimensions of the standard baffle used in the experiments (unit: mm).

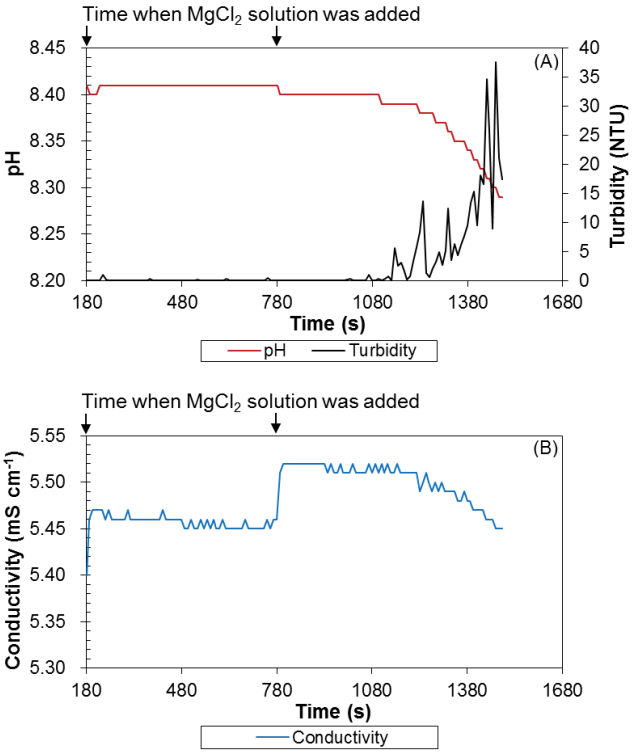

Fig. S2. Changes in pH, turbidity (a), and conductivity (b) of the solution in the stirred beaker during Exp. 14 at pH 8.4 (Conditions: addition volume of $MgCl_2$ solution = 10 mL, addition interval of $MgCl_2$ solution = 10 min, agitation rate = 400 rpm, no seeds).

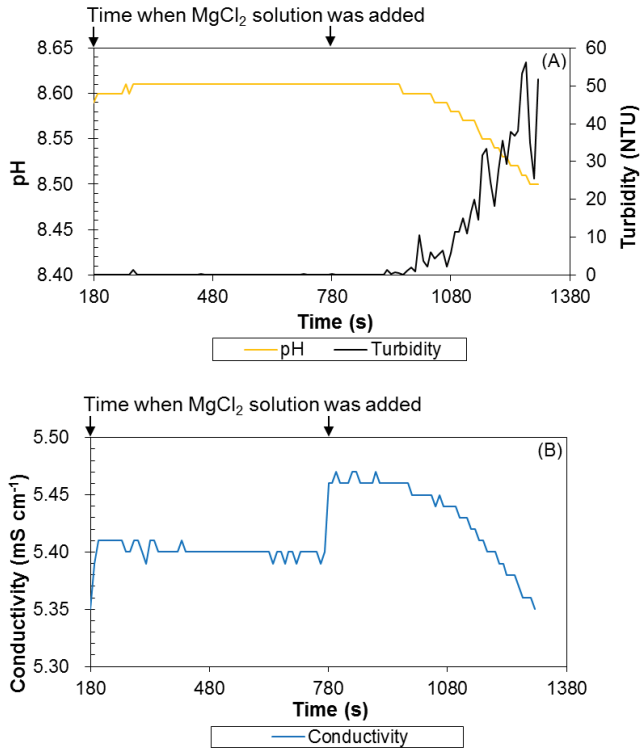

Fig. S3. Changes in pH, turbidity (a), and conductivity (b) of the solution in the stirred beaker during Exp. 15 at pH 8.6 (Conditions: addition volume of $MgCl_2$ solution = 10 mL, addition interval of $MgCl_2$ solution = 10 min, agitation rate = 400 rpm, no seeds).